Farsighter: Efficient Multi-Step Exploration for Deep Reinforcement Learning

Yongshuai Liu and Xin Liu

Department of Compute Science, University of California, Davis, CA, U.S.A.

Abstract: Uncertainty-based exploration in deep reinforcement learning (RL) and deep multi-agent reinforcement learning (MARL) plays a key role in improving sample efficiency and boosting total reward. Uncertainty-based exploration methods often measure the uncertainty (variance) of the value function; However, existing exploration strategies either underestimate the uncertainty by only considering the local uncertainty of the next immediate reward or estimate the uncertainty by propagating the uncertainty for all the remaining steps in an episode. Neither approach can explicitly control the bias-variance trade-off of the value function. In this paper, we propose Farsighter, an explicit multi-step uncertainty exploration framework. Specifically, Farsighter considers the uncertainty of exact k future steps and it can adaptively adjust k. In practice, we learn Bayesian posterior over Q-function in discrete cases and over action in continuous cases to approximate uncertainty in each step and recursively deploy Thompson sampling on the learned posterior distribution with TD(k) update. Our method can work on general tasks with high/low-dimensional states, discrete/continuous actions, and sparse/dense rewards. Empirical evaluations show that Farsighter outperforms SOTA explorations on a wide range of Atari games, robotic manipulation tasks, and general RL tasks.

1 INTRODUCTION

Deep reinforcement learning (DRL) and deep multi-agent reinforcement learning (MARL) have shown great performance in tasks such as robots (Yang and Gu, 2004) and Atari games (Mnih et al., 2015), etc. They are also promising methods for problems such as biometrics (Lu and Liu, 2015; Lu et al., 2017; Qu et al., 2015) and security (Liu et al., 2018). However, sample inefficiency remains to be a significant barrier to applying DRL and MARL in real-world applications (Liu and Liu, 2023b; Liu and Liu, 2021; Liu et al., 2020a). One bottleneck is the exploration problem, which can be even more challenging in complex environments with sparse rewards, noisy distractions, long horizons, and nonstationary co-learners.

Recently, the uncertainty-based exploration strategies (Yang et al., 2021; Liu and Liu, 2023a) are proposed in DRL to tackle the above problems. Such strategies estimate the uncertainty (variance) of Q values via Bayesian posterior and incentivizes actions based on its uncertainty. Those approaches can be directly extended to the multi-agent problem as well (Zhu et al., 2020). However, the majority of existing approaches (Osband et al., 2016; Janz et al.,

2019) easily *underestimate* the uncertainty by only considering the local uncertainty of next step's immediate reward, e.g., BDQN (Azizzadenesheli et al., 2018), and thus remain inadequate. First, none of them works very well on the tasks with sparse rewards, e.g., Skiing. Futhermore, these methods introduce a new uncertainty vanishing issue (Ecoffet et al., 2019): as an agent explores the environment and becomes familiar with a local area after a number of steps, the uncertainty of the area diminishes, thus the agent loses its exploration ability and may get stuck in a local area. Because of those problems, the agent usually cannot explore the environment enough which causes the Q-value estimation to be biased. To address the problems, UBE (O'Donoghue et al., 2018), OB2I (Bai et al., 2021), WQL (Metelli et al., 2019) argue that, to achieve effective exploration, it is necessary that the uncertainty about each Q value, quantified by its variance, is equal to the uncertainty about the next step's immediate reward and the next state's Q value. Thus, the new family of algorithms propagate the uncertainty in a long-term manner: they accumulate uncertainties for all the remaining steps in an episode. However, because the environments usually contain thousands of steps, this ap-

proach tends to have *too large uncertainty (variance)*, e.g., the OB2I estimation in Atari games. Both the local uncertainty and uncertainty propagation methods lack the ability to *explicitly* adjust the number of future uncertainty steps to be considered and thus it is difficult to use them to explicitly control the bias-variance(uncertainty) trade-off of the Q function.

To address this challenge, we propose Farsighter, an explicit multi-step uncertainty exploration framework in DRL, to balance the bias-variance of Q estimation. Farsighter considers the uncertainty for k future steps, whose value can be explicitly adjusted to balance the bias-variance trade-off of Q estimation. Compared to the "one-step" local uncertainty methods, it is beneficial in cases with long-term sparse rewards. The agent learns the impact of the current action on future k-step rewards even if no immediate reward is given. Moreover, considering k-step future uncertainties helps escape the local familiar areas, thus alleviating the uncertainty vanishing issue. Compared to the uncertainty propagation methods, Farsighter is capable to rightly estimate the uncertainty with an suitable step value k, which is adjustable.

Specifically, Farsighter learns Bayesian posterior over Q-function/action to approximate uncertainty in both discrete and continuous action tasks. For discrete action tasks, we deploy the value-based DDQN (Van Hasselt et al., 2016) and use Bayesian linear regression for the last layer of the Q-network to approximate the Bayesian posterior over Q-function. For continuous action tasks, we build on NAF (Gu et al., 2016), and use the Bayesian Neural network to approximate the Bayesian posterior over actions of the Q-function. This allows us to directly incorporate the uncertainty over the Q-function in each step. To estimate the "k-step" uncertainty in practice without exponential computational complexity, we formulate the problem as a recursive Gaussian process and perform TD(k) update instead of TD(0), in which we recursively deploy Thompson sampling on the learned posterior distributions for k steps.

In summary, we make the following contributions:

- We propose Farsighter that allows explicit k-step uncertainty exploration to balance the bias and variance trade-off of Q values. Moreover, we also develop an adaptive Farsighter to further improve the exploration performance.

- We develop Farsighter implementations in both discrete and continuous action tasks. It can also apply on a wide range of RL tasks with high/low-dimensional states and sparse/dense rewards.

- Empirical results show that Farsighter outperforms SOTA in high-dimensional Atari games and continuous control robotic tasks.

2 RELATED WORK

Uncertainty-based methods usually model the uncertainty of the Q function via the Bayesian posterior. The agent is encouraged to explore the unknown environment with high uncertainty.

The majority of existing exploration approaches consider the local uncertainty of next immediate reward. RLSVI (Osband et al., 2016) performs Bayesian regression in linear MDPs so that it can sample the value function through Thompson Sampling. BDQN (Azizzadenesheli et al., 2018) performs Bayesian Linear Regression (BLR) in the last layer of the Q-network. It approximately considers the last-layer Q-network as a linear MDP problem. Successor Uncertainty (Janz et al., 2019) approximates the posterior through successor features which are linear to the Q value of the corresponding state-action pairs.

The above methods only consider the local uncertainty in next one-step. Nevertheless, some other methods propagate the uncertainty with all the remaining steps in an episode. For example, UBE (O'Donoghue et al., 2018) proposes to learn the uncertainty with Uncertainty Bellman Equation. WQL (Metelli et al., 2019) approximates the parametric posterior distribution based on Wasserstein barycenters. OB2I (Bai et al., 2021) performs backward induction of bootstrapped-based uncertainty to capture the long-term uncertainty in an whole episode. Although those methods also propagate the uncertainty in a multi-step manner, which can alleviate the uncertainty vanishing issue as well, they usually have too large uncertainty in long-horizon cases (e.g., Atari Games). Thus we propose Farsighter in the next sections, which can explicitly balance the bias-variance of the Q-estimation.

3 PRELIMINARIES

3.1 Markov Decision Process (MDP)

A MDP is represented by the tuple (S, A, R, P, γ) (Liu et al., 2021a; Liu et al., 2021b; Liu et al., 2021c), where S is the set of states; A is the set of actions; R is the reward function; P is the transition probability function and γ is the reward discount factor. The objective of an MDP is to learn a policy π to maximize the discounted cumulative reward. Given a state s and action a, the Q function is

$$Q(s,a) = \mathbb{E}_{\tau \sim \pi}[\sum_{t=0}^{\infty} \gamma^t R(s_t, a_t, s_{t+1}) | s_0 = s, a_0 = a].$$

Following the Bellman equation in MDPs, we

have the Q-function

$$Q(s_t, a_t) = R_{s_t}^{a_t} +$$
$$\gamma \sum_{s_{t+1} \in S} P_{s_t s_{t+1}}^{a_t} \sum_{a_{t+1} \in A} \pi(a_{t+1}|s_{t+1}) Q(s_{t+1}, a_{t+1}). \quad (1)$$

3.2 Double Deep Q Networks (DDQN)

For discrete action tasks, we build our algorithm on the value-based DDQN (Van Hasselt et al., 2016), which is an extension of DQN (Mnih et al., 2015). DDQN uses two identical neural network models. One learns during the experience replay, just like DQN, and the other one, called target network Q^{target}, is a copy of the last episode of the first model. The core of DDQN is to learn the Q-function through minimizing a surrogate to Bellman residual (Antos et al., 2008) using temporal difference (TD) update (Tesauro et al., 1995).

Given a consecutive experience tuple (s, a, r, s'), the target value is

$$y = r + \gamma Q(s', \arg\max_{a'} Q(s', a', \theta), \theta^{target}). \quad (2)$$

DDQN learns the Q function by approaching the empirical estimates of the following regression loss:

$$L(Q, Q^{target}) = \mathbb{E}[(Q(s,a) - y)^2]. \quad (3)$$

Moreover, the parameters of the target network Q^{target} are updated frequently by copying the parameters of the learning network Q.

3.3 Normalized Advantage Function (NAF)

Value-Based methods, like DDQN, suit problems with discrete action spaces. NAF is designed for continuous action-space tasks. The idea behind NAF is to let the maximization of the Q function be determined during the Q-learning update. Specifically, instead of having one output stream from the Q-network, NAF has three streams. One stream estimates the value function $V(s|\theta^V)$ (parameterized by θ^V), and another estimates the Advantage $A(s,a|\theta^A)$ (parameterized by θ^A), which is further parameterized as a quadratic function based on action $\mu(s|\theta^a)$ (parameterized by θ^a) and matrix P. Combined together, we estimate Q-Values as:

$$Q(s,a) = A(s,a|\theta^A) + V(s|\theta^V),$$
$$A(s,a|\theta^A) = -\frac{1}{2}(a - \mu(s|\theta^a))^T P(s|\theta^P)(a - \mu(s|\theta^a)). \quad (4)$$

$P(s|\theta^P)$ is a state-dependent, positive-definite square matrix, which is parametrized by $P(s|\theta^P) =$

$L(s|\theta^P)L(s|\theta^P)^T$. L is a lower-triangular matrix, where the diagonal terms are exponentiated. Since the Q-function is quadratic in action a, the action that maximizes the Q-function is always given by $\mu(s|\theta^a)$. NAF updates the parameter based on the rule of DDQN (Eq. 3). The different between those two methods is how to select action in each step.

4 FARSIGHTER: MULTI-STEP EXPLORATION

In this section, we introduce Farsighter that performs exploration by considering the uncertainty of the next "k-step". In Sec. 4.1, we formulate the multi-step uncertainty estimation problem. In Sec. 4.2 and 4.3, we present how to estimate uncertainty with discrete actions and continuous actions in each step. In Sec. 4.4, we introduce how to perform multi-step exploration. Last, in Sec. 4.5, we show how to adaptive choose the number of k.

4.1 Problem Formulation

Assume the ground truth of a Q-value is Q_g. we define the Bayesian posterior of a Q-estimation as $\mathcal{N}(Q_e, \varepsilon)$, where Q_e is the mean value and ε is the variance of the Q-estimation. We call the distance of $|Q_g - Q_e|$ as the bias of the Q-estimation and ε is the uncertainty.

The uncertainty of Q-estimation ε follows the uncertainty Bellman equation (Theorem 1 of UBE (O'Donoghue et al., 2018)):

$$\varepsilon(s_t, a_t) = \delta_{s_t}^{a_t} +$$
$$\gamma \sum_{s_{t+1} \in S} P_{s_t s_{t+1}}^{a_t} \sum_{a_{t+1} \in A} \pi(a_{t+1}|s_{t+1}) \varepsilon(s_{t+1}, a_{t+1}), \quad (5)$$

for all (s,a) and $t = 1, ..., T$, where $\varepsilon^{T+1} = 0$ and where we call $\delta_{s_t}^{a_t}$ the local uncertainty at (s_t, a_t).

In "one-step" uncertainty estimation methods (e.g., BDQN), the uncertainty of the Q estimation only contains the local uncertainty, thus $\varepsilon(s_t, a_t) = \delta_{s_t}^{a_t}$. Empirically, the local "one-step" uncertainty is usually small and it is easy to be vanished, which leads the agent cannot explore the environment enough. Not exploring enough results the Q-estimation usually has high bias. On the other hand, in uncertainty propagation methods (e.g., OB2I), which propagate all the remaining uncertainty in an episode (Eq. 5 can be unfolded to T steps), the variance ε is usually very large. Hence, the Q estimation exhibits high uncertainty and the agent can explore more in the environment. In such cases, the Q-estimation is usually less biased, however, large variance is at the

risk of too much unnecessary exploration and thus slow down the learning convergence. Thus we need a method that explicitly adjust the uncertainty exploration steps k that balance the bias-variance trade-off. The uncertainty we use in Farsighter is:

$$\varepsilon(s_t, a_t) = \delta_{s_t}^{a_t} + ... + $$
$$\gamma^k \sum_{s_{t+k} \in S} P_{s_t s_{t+k}}^{a_k} \sum_{a_{t+k} \in A} \pi(a_{t+k}|s_{t+k}) \delta(s_{t+k}, a_{t+k}). \quad (6)$$

In Sec. 5.1, we empirically demonstrate the benefits of Farsighter.

4.2 Estimating Bayesian Uncertainty with Discrete Actions

For discrete action cases, we build our algorithm on the DDQN and estimate the uncertainty of the Q-function. DDQN architecture consists of a deep neural network where the last layer is usually a linear MLP function of the state representation and action. Thus, given any state s and action a, $Q(s,a) = \phi_\theta(s)^T \omega_a$, where $\phi_\theta(s) \in \mathbb{R}^d$ parameterized by θ represents state s and $\omega_a \in \mathbb{R}^d$ is the parameter of the last linear MLP layer on action a.

To estimate the uncertainty, we build Farsighter over DDQN with Bayesian framework. In the last layer of Q-network $Q(s,a)$, instead of using the linear MLP regression, Farsighter deploys the Gaussian Bayesian linear regression (BLR) (Rasmussen, 2003), which results in an approximated Bayesian posterior on the ω_a and consequently on the Q-function. The Bayesian posterior ω_a is modeled as Gaussian with $\{\bar{\omega}_a, Cov_a\}$, where $\bar{\omega}_a$ is the posterior mean and Cov_a is the posterior covariance. Moreover, we leverage the re-parameterization trick to write

$$Q(s,a) = \phi_\theta(s)^T \omega_a = \phi_\theta(s)^T(\bar{\omega}_a + \sqrt{Cov_a}z), \quad (7)$$

where z is a random variable $z \sim \mathcal{N}(0,I)$. Through BLR, the agent efficiently captures the uncertainty over the Q estimates. In practice, the algorithm takes as input $\phi_\theta(s)$ which has two output 'heads', one which is attempting to learn the optimal Q-values as normal DDQN, the other is attempting to learn the uncertainty values of the Q estimation. In other words,

$$Q(s,a) = Q_\theta(s,a) + \phi_\theta(s)^T \sqrt{Cov_a}z, \quad (8)$$

In the parameter updating process, the BLR-based Q-function updates parameters θ and ω_a separately. The process is shown in the Algorithm 1.

Update θ: We fix the head ω_a and update θ using the normal head following the standard DDQN (Eq. 3).

Update $\bar{\omega}_a, Cov_a$: we update $\bar{\omega}_a$ and Cov_a with fixed $\phi_\theta(s)$. Given a dataset $\mathcal{D} = \{s_i, a_i, y_i\}_{i=1}^D$, where

y_i are target values, we construct $|\mathcal{A}|$ disjoint datasets for each action, $\mathcal{D} = \cup_{a \in \mathcal{A}} \mathcal{D}_a$, where $\mathcal{D}_a$ is a set of tuples (s_i, a_i, y_i) with the action $a_i = a$. Let us construct a matrix $\Phi_a \in \mathbb{R}^{d \times D_a}$, a concatenation of feature column vectors $\{\phi(s_i)\}_{i=1}^{D_a}$, and $\mathbf{y}_a \in \mathbb{R}^{D_a}$, a concatenation of target values in set $\mathcal{D}_a$. We then approximate the posterior distribution of ω_a as follows

$$\bar{\omega}_a = \frac{1}{\sigma_\varepsilon^2} Cov_a \Phi_a \mathbf{y}_a, \quad Cov_a = \left(\frac{1}{\sigma_\varepsilon^2}\Phi_a \Phi_a^\top + \frac{1}{\sigma^2}I\right)^{-1}, \quad (9)$$

where $I \in \mathbb{R}^d$ is an identity matrix. This is the derivation of the BLR, with zero mean prior and as σ and σ_ε^2 as the variance of prior and likelihood respectively.

4.3 Estimating Bayesian Uncertainty with Continuous Actions

Value-Based methods, like DDQN, suit problems with discrete action spaces. For continuous action cases, we build our algorithm on the NAF and estimate the uncertainty on actions. NAF architecture consists three output streams $\mu(s|\theta^a), L(s|\theta^P)$, and $V(s|\theta^V)$, as shown in Eq. 4. Usually, the three sub-networks are functions of a shared state representation network $\phi_\theta(s)$. Thus, we have $\mu(s|\theta^a) = \mu(\phi(s)|\theta^a)$, where θ^a is the parameter of layers taking state representation $\phi(s)$ as input and output action a.

The Original NAF cannot estimate the uncertainty for actions. Therefore, in our work, we *first* propose to estimate the exploration uncertainty for continuous actions using a Bayesian neural network (BNN) (Kononenko, 1989) for the action sub-network, $\mu(\phi(s)|\theta^{va})$. BNN treats the model weights and output action as variables. Instead of finding a set of optimal estimates, BNN fits the Bayesian posterior distributions for them. Every weight in θ^{va} is modeled as a Gaussian distribution with a mean and variance. It directly learns the uncertainties of the actions given a state representation $\phi(s)$. To get action, we can sample one set of weights from the distribution. In practice, our new architecture consists four output streams, $\mu(s|\theta^{va}), \mu(s|\theta^a), L(s|\theta^P)$, and $V(s|\theta^V)$, where $\mu(s|\theta^{va})$ leans the BNN of actions. To update the parameters, we update parameters of $\theta^a, \theta^V, \theta^P, \theta$ and θ^{va} separately.

Update $\theta^a, \theta^V, \theta^P, \theta$: we update $\theta^a, \theta^V, \theta^P, \theta$ with a fixed θ^{va} and update them with the normal NAF.

Update θ^{va}: to learn the posterior distribution $\mu(\theta^{va}|(\phi(s),a))$, we fix the parameters of $(\theta^a, \theta^V, \theta^P, \theta)$ and update the parameters of θ^{va} with the Evidence Lower Bound(ELBO) loss (Kononenko, 1989). Specifically, we approximate the posterior distribution $\mu(\theta^{va}|(\phi(s),a))$ with another distribution

$\hat{\mu}(\theta^{va})$, which is called a variational distribution. We further minimize the KL divergence between them $D_{KL}(\hat{\mu}(\theta^{va})||\mu(\theta^{va}|(\phi(s),a)))$. Based on the variational inference theory (Blei et al., 2017), we get the ELBO loss:

$$D_{KL}(\hat{\mu}(\theta^{va})||\mu(\theta^{va})) - \mathbb{E}_{\theta^{va}\sim\hat{\mu}}[\log\mu(a|s,\theta^{va})] \quad (10)$$

Note that we use BNN for continuous action tasks and BLR for discrete ones. BNN has better performance but at the cost of higher computation complexity. Because the dimension of state representation is typically low for continuous action tasks, e.g., robotic manipulation tasks, we consider it computationally acceptable. In comparison, as discussed in the appendix, BLR does not increase the computation complexity compared to MLP. It is suitable when the dimension of state representation is high, and thus we choose it for discrete action tasks.

4.4 Exploration with Multi-Step Uncertainty

In Sec. 4.2 and 4.3, we show how to estimate the uncertainty. Each step is a Gaussian process with a posterior on Q-function/actions. For example, in discrete cases, the GP posterior applies on the ω_a (Eq. 8) and consequently on the Q-function. In each step, we can sample an instance from the posterior. Since each step has different GP posteriors based on different states and actions, these nested expectations are analytically intractable; we cannot directly calculate the "k-step" uncertainty distribution. Moreover, the number of instances in the recursive Gaussian process grows exponentially in the horizon k. Therefore, considering all the possible roll-outs in k steps is computationally difficult. To address it, we formulate the "k-step" process as a recursive Gaussian process and perform TD(k) update instead of TD(0). More specifically, we recursively deploy Thompson sampling on the learned posterior distributions for k steps to approximate the k-step uncertainty (Eq. 6), which means the Q-function becomes

$$Q(s_t,a_t) = \mathbb{E}_{\tau\sim\pi}[R(s_t,a_t,s_{t+1}) + \gamma R(s_{t+1},a_{t+1},s_{t+2})$$
$$+ ... + \gamma^k \max_{a_{t+k}\in A} Q^*(s_{t+k},a_{t+k})|s_t,a_t]$$

For discrete action cases, we sample a random variable z for Eq. 8 in each step and obtain a deterministic Q-function. Given the deterministic Q-function, we can decide which action maximizes the Q values. For continuous action cases, we sample a variance ε from the BNN posterior $\mu(s|\theta^{va})$ in each step and then directly get action $\mu(s|\theta^a) + \varepsilon$ from the sampled weights . After taking the action, we go to the next

---

Algorithm 1: Farsigher: Multi-step Exploration.

Initialize θ, θ^{target}, k, Q-variance target $\check{\varepsilon}$, and $\forall a, \bar{\omega}_a, Cov_a, \bar{\omega}_a^{target}$; Replay buffer $RB = \{\}$

1: **for** t=0, k, 2k, 3k... **do**
2:    $\{r^k, s_{t+k}\}$ = K-STEP$(s_t, \theta, \bar{\omega}_a, \sqrt{Cov_a}, \gamma, r^k = 0, itr = 0)$
3:    Store $\{s_t, a_t, r^k, s_{t+k}\}$ into replay buffer RB
4:    Sample a mini-batch $\{s_i, a_i, r^k, s_{i+k}\}$ from the latest N steps to alleviate off-policyness bias
5:    Update the parameters of θ with DDQN, where $r = r^k, s' = s_{i+k}$ and keep $\bar{\omega}_a, Cov_a$ fixed
6:    Every M steps: Update the GP posterior $\{\bar{\omega}_a, Cov_a\}$ for all actions
7:       **if** Q-variance $< \check{\varepsilon}$: k+=1; Empty RB.
      else if Q-variance $> \check{\varepsilon}$: k-=1; Empty RB.
8:    Every N steps: reset $\theta^{target} = \theta, \bar{\omega}_a^{target} = \bar{\omega}_a$
9: **end for**

Algorithm 2: K-STEP$(s_t, \theta, \bar{\omega}_a, \sqrt{Cov_a}, \gamma, r^k, itr)$.

Input: s_t it the current state; $\theta, \bar{\omega}_a$ and Cov_a are parameters of Q-function, γ is the discounted factor; r^k is the discounted sum of k-step rewards; itr is the number of steps in the k loop.
Output: the discounted sum of k-step rewards r^k and the last state after k steps.

1: **if** itr=k: **return** r^k, s_{t+1}
2: Sample $z_t \sim N(0,I)$ and then get a deterministic $Q(s,a) = Q_\theta(s,a) + \phi_\theta(s)^T \sqrt{Cov_a} z_t$
3: Take action $a_t = \arg\max_a Q(s,a)$
4: Get next state s_{t+1} and reward r_t by interacting with the environment.
5: $r^k += \gamma^{itr} * r_t$
6: **return** K-STEP$(s_{t+1}, \theta, \bar{\omega}_a, \sqrt{Cov_a}, \gamma, r^k, itr+1)$

---

state from the environment. As shown in Algorithm 2, we recursively deploy the process for k steps and get the last state s_{t+k} and the discounted sum of k-step rewards r^k, where the k-step uncertainties information is stored.

The pseudocode of the whole learning process for discrete action cases is shown in Algorithm 1. Instead of saving the one-step state and action tuple, we get k-step state s_{t+k} and reward r^k from Algorithm 2. For continuous action cases, the workflow is similar to discrete action cases; we provide the pseudocode in the Appendix. For multi-step updates, we keep the update rule same as one-step updates as mentioned in Sec. 4.2 and 4.3. We only change the way to calculate the target value, $y = r + \gamma^k Q(s', \arg\max_{a'} Q(s',a',\theta), \theta^{target})$, where r is the
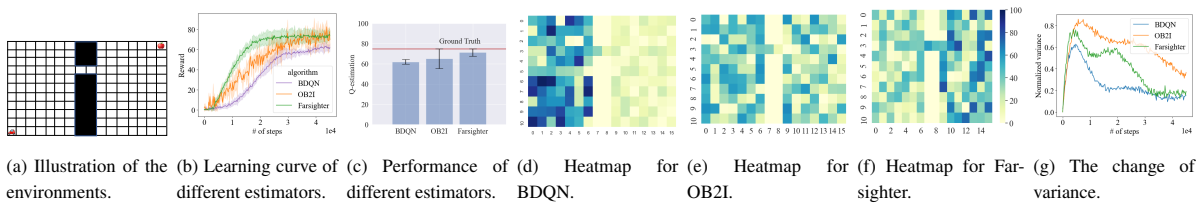
(a) Illustration of the environments. (b) Learning curve of different estimators. (c) Performance of different estimators. (d) Heatmap for BDQN. (e) Heatmap for OB2I. (f) Heatmap for Farsighter. (g) The change of variance.

Figure 1: Validation of the effectiveness of multi-step uncertainty.

discounted sum of k-step rewards r^k and s' is the last state after k steps s_{t+k}. Thus, our multi-step uncertainty estimation would not increase the computation and the memory complexity. Moreover, to alleviate the bias introduced by off-policyness in multi-step learning, the network is trained using the latest N-step samples, where N is the target network update period, as suggested in (Mnih et al., 2016). In addition, since the k-step reward and state are obtained from recursive Thompson sampling and they contain the uncertainty information of the future k steps, the learned Q function also contains the uncertainty information, which is represented on the variance of the posterior. The variance helps us quantify the uncertain impact of the next k-step in turn.

4.5 Adaptive K

Empirically, to learn a good policy as soon as possible, it is desirable to have more exploration at the beginning stage and then gradually decrease exploration to increase exploitation. As shown above, the amount of uncertainty is represented by the variance of the Bayesian posterior (Eq. 6). In principle, we can set a large initial k to enlarge the exploration at the beginning stage and then set posterior variance target to mantain a certain level of exploration. Based on this intuition, we have developed an adaptive Farsighter. In the adaptive Farsighter, we initial k to be a large number and set a target to the variance. If the variance is smaller than the target, we increase k, otherwise, we decrease it. In this manner, the agent can keep exploring the environment. The pseudocode for discrete action cases is shown in the Algorithm 1. We show the affects of different k in Sec. 5.3.

5 EXPERIMENTS

In this section, we investigate the following properties of Farsighter: 1) We illustrate the insight of multi-step uncertainty exploration using a toy example, 2) We compare the performance of Farsighter with SOTA, on a large range of RL tasks, including Atari games and continuous control tasks, and 3) We investigate the effect of a different number of future steps.

5.1 K-Step Uncertainty Insight

To illustrate the idea of multi-step uncertainty, we design a toy maze task as shown in Fig. 1a. The agent (car) starts from the bottom left corner. In each step, the car can go either up, down, left, or right. The car wants to get the apple (top right corner) and it cannot pass the black wall area. The bridge is the only way that connects the left and right sides. The reward is 100 if the car reaches the apple, and -1 otherwise each step.

We further compare the local uncertainty exploration (e.g., BDQN), uncertainty propagation (e.g., OB2I) and k-step uncertainty exploration(Farsighter) under same interaction steps, 40k, where all algorithms have converged, as shown in Fig 1b. The optimal Q-value Q_g for the car from the bottom left corner is 75. From Fig. 1c, we can see that the Q-estimation of BDQN is highly biased, as we discussed in Sec. 4.1: the mean is around 62 which is far from the optimal 75 and the variance is low. On the other hand, the OB2I Q-estimation is less biased, but the variance of OB2I Q-estimation is very large. In comparison, the bias of Farsighter is the smallest and the variance is lower than OB2I.

In addition, we show the heatmap of the number of state visited times during learning process for BDQN (Fig. 1d), OB2I(Fig. 1e), and Farsighter (Fig. 1f) . For BDQN, fewer visits occur on the right side of the map and most of the interactions remain on the left side because the car does not cross the bridge often enough and repeatedly explore the left familiar side (uncertainty vanishing). On the other hand, it is easier for the car to cross the bridge with OB2I and Farsighter. More visits occur on the right, which enhances the car reaching to the apple more frequently. However, OB2I performs too much exploration, which can be observed from the action selection process where action varies in the same state, e.g., all the episode traces are different even with same Bayesian Q function. The visited times for both sides are similar. In comparison, Farsighter visits more on the right and frequently reaches the apple, since in the later learning

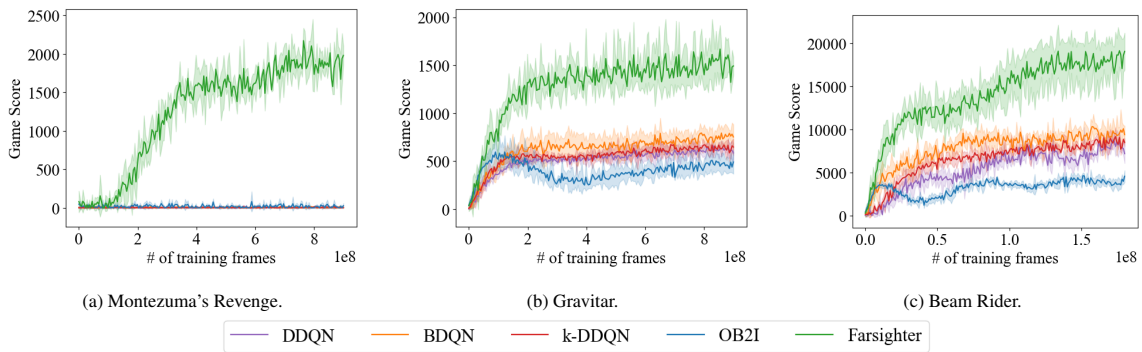(a) Montezuma's Revenge.   (b) Gravitar.   (c) Beam Rider.

Figure 2: The game score for Atari Games.

phase the policy has converged and the agent leans to access the right side. Intuitively, multi-step uncertainty explorations (Farsighter and OB2I) consider more exploration for further locations. When the car is at the bridge, it is easier to find the new locations on the right, which encourages the car to explore more on the right side. In comparison, the one-step agent (BDQN) takes the left as the local optima area and sticks to it more often. Thus the Q-estimation is biased since the agent cannot explore the environment enough. However, the OB2I performs too much exploration, since the variance is high, which leads to slow converge speed. Farsighter balances the bias-variance trade-off by explicitly choosing an appropriate k.

Moreover, we also study the changes of posterior variance among these exploration methods in Fig. 1g. In the beginning, variances are low because the networks are randomly initialized. When the learning starts, the variances increase rapidly to award exploration. After that, the posterior variance in BDQN gradually decreases because as the agent gathers more samples, the uncertainty is vanishing. In comparison, in the Farsighter, even the posterior variance decreases as well earlier, it becomes larger later on (because the agent accesses more states on the right side) and then decreases finally when the learning is converged. The results show that Farsighter alleviates the uncertainty vanishing problem because Farsighter learns high uncertainties on the right side by considering future steps. The OB2I can also help to alleviate the uncertainty vanishing. But it is hard to converge, since the variance is high.

5.2 Exploration Performance

Environments: Farsighter can work on a wide range of RL tasks with high/low-dimensional states, discrete/continuous actions, and sparse/dense rewards. We empirically study Farsighter on a variety of

Atari games in the Arcade Learning Environment (ALE) (Bellemare et al., 2013) and robotic control tasks using MuJoCo physics engine (Liu et al., 2020b). The states in ALE are high-dimensional images and the action space is discrete. In comparison, the robotic control tasks are in low-dimension but the action space is continuous. We evaluate Farsighter on 49 Atari suite of games including hard-explored games with sparse rewards (e.g., Montezuma's Revenge, Gravitar, and Venture) and games with dense rewards (e.g., Beam Rider, Atlantis, and Freeway); two challenging robot control tasks (FetchPickAndPlace and HandManipulateBlock) with sparse rewards and a control task (Walker2D) with dense rewards.

Baselines: We compare Farsighter to four baselines in discrete action environments: DDQN with ε-greedy exploration and BDQN, a parametric posterior based exploration, which only considers one-step uncertainty. Moreover, to study the effects of multi-step learning, we also compare Farsighter with 'k-DDQN' which uses ε-greedy exploration in each step but considers k steps. We also compare with OB2I, which is the SOTA uncertainty propagation method that use non-parametric posterior based exploration. Similarly, for continuous control tasks, we select three baselines: standard one-step NAF with random exploration, multi-step NAF with random exploration, one-step NAF with Bayesian uncertainty exploration. To be fair, we keep the shared parts of the methods to be the same for different exploration methods, e.g., the state representation layers, and the hyper-parameters.

Performance: Farsighter outperforms DDQN, BDQN and OB2I in 36 out of 49 Atari games. We show parts of the evaluation results in Fig. 2 and Fig. 5. More detailed results (e.g., game scores for 49 Atari games) are available in the appendix. We run each experiment 10 times with different random seeds and show the average performance. The shaded area is the standard deviation in the Figures.
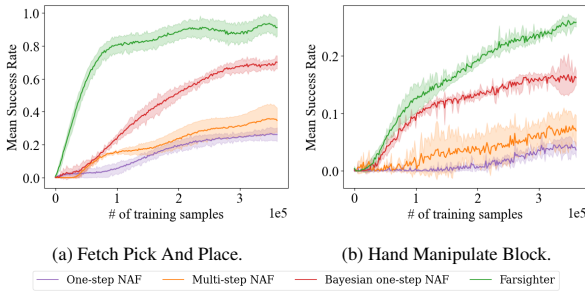
(a) Fetch Pick And Place.   (b) Hand Manipulate Block.

One-step NAF — Multi-step NAF — Bayesian one-step NAF — Farsighter

Figure 5: The mean success rate for continue robotic tasks.

Figure 3: The effects of different uncertainty steps in Montezuma's Revenge.

Figure 4: The effects of different initial k and uncertainty target.

Figure 2 compares the game scores with the four baselines in Atari Games. Farsighter achieves higher scores substantially. In the notoriously hard exploration game Montezuma's Revenge, Farsighter achieve positive results, while others achieve zero score. The reason is that we initial k=150, which accumulates the uncertainty over k timesteps before performing an update. A higher initial k leads to the agent to explore more in the game and encounter informative state faster. other methods (e.g., BDQN, DDQN) cannot explore enough in the game and most of the reward feedback is zero, thus it is hard to get positive score. On the contrary, OB2I performs prodigious exploration because the uncertainty is very large in Atari Games with thousands of steps, which results in the agent almost taking random actions and hard to get positive rewards. In Gravitar and Beam Rider, DDQN and BDQN show comparable performance. BDQN performs a little better since the agent can explore with one-step uncertainty and k-DDQN cannot improve the performance compared with DDQN, which means k-step learning without uncertainty cannot improve the exploration either. Interestingly, the OB2I increases faster at early and then degenerates. This is because OB2I performs unnecessary exploration which may guide a direction that is unrelated to the environment reward. In comparison, Farsighter performs enough exploration and exploit it efficiently.

Figure 5 shows the performance comparison for continuous robotic tasks. The results show that the multi-step uncertainty exploration also outperforms one-step uncertainty exploration and random exploration in continuous action tasks. In the Fetch-PickAndPlace task, Farsighter achieves almost 100% success rate and it only takes around 100 million steps. The success rate in HandManipulateBlock is also the best and it takes the least samples for the sample success rate. Overall, we can conclude that Farsighter is an effective exploration method by considering multi-step uncertainty and it works on general RL tasks.
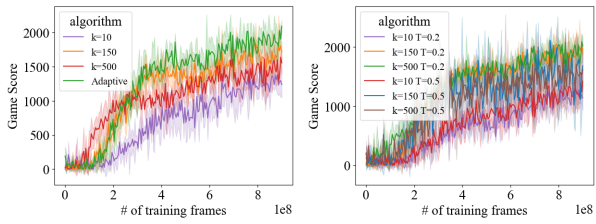
5.3 The Impact of K

Figure 3 shows the impact of k in Montezuma's Revenge, where the performance increases with k initially and then drops, with $k = 150$ achieving the best score. This trend exists for other environments although the optimal k value varies. An interesting observation is that the increased velocity of the scores at the earlier stage is positively proportional to the number of uncertainty steps. This illustrates the importance, in particular in the early stages, of multi-step exploration. The number of uncertainty steps is a trade-off between exploitation and exploration. When k is large, (e.g., k=500), the agent considers more cumulative uncertainty, and large uncertainty forces the agent to explore more about the environment, which could be desirable in the early stages, but at the risk of too much exploration and thus difficulties in convergence. This might explain why uncertainty propagation methods (e.g., OB2I, WQL) which accumulate uncertainties for all the remaining steps in an episode are outperformed by our method. On the contrary, when k is small (e.g., k=10), the agent only considers the uncertainty of the next few steps. The uncertainty is easy to vanish and the agent tends to exploit.

Farsighter can explicitly balance the bias-variance trade-off by adjusting the number of k. As discussed in Sec. 4.5, we can use an adaptive k by seting a variance target. From Fig. 3, we can see the adaptive Farsighter achieves the best result, where the score increases quickly initially and also finishes with the highest value. Moreover, in Fig. 4, we show the impact of different initial k and variance target. When the initial k is too small, e.g., 10, Farsighter performs worst, since the exploration is not enough even though the k is increasing to catch up with the variance target. On the contrary, when the initial k is large enough (e.g., 150, 500), the initial exploration is adequate. A suitable variance target that maintains the exploration to a certain level in the learning process can increase the performance, such as in the Montezuma's Revenge, the variance target 0.2 outperforms 0.5.

6 CONCLUSION

In this paper, we propose Farsighter, an multi-step uncertainty exploration framework in DRL and we can explicitly adjust the number of future steps to balance the Q-estimation bias-variance trade-off. Farsighter helps to alleviate the sparse reward and uncertainty vanishing problem. Moreover, it avoids the uncertainty to be too large in the uncertainty propagation methods. It outperforms SOTA on a wide range of RL tasks with high/low-dimensional states, discrete/continuous actions, and sparse/dense rewards, including high-dimensional Atari games and continuous control robotic manipulation tasks.

ACKNOWLEDGEMENTS

REFERENCES

Antos, A., Szepesvári, C., and Munos, R. (2008). Learning near-optimal policies with bellman-residual minimization based fitted policy iteration and a single sample path. *Machine Learning*, 71(1):89–129.

Azizzadenesheli, K., Brunskill, E., and Anandkumar, A. (2018). Efficient exploration through bayesian deep q-networks. In *2018 Information Theory and Applications Workshop (ITA)*, pages 1–9. IEEE.

Bai, C., Wang, L., Han, L., Hao, J., Garg, A., Liu, P., and Wang, Z. (2021). Principled exploration via optimistic bootstrapping and backward induction. In *International Conference on Machine Learning*, pages 577–587. PMLR.

Bellemare, M. G., Naddaf, Y., Veness, J., and Bowling, M. (2013). The arcade learning environment: An evaluation platform for general agents. *Journal of Artificial Intelligence Research*, 47:253–279.

Blei, D. M., Kucukelbir, A., and McAuliffe, J. D. (2017). Variational inference: A review for statisticians. *Journal of the American statistical Association*, 112(518):859–877.

Ecoffet, A., Huizinga, J., Lehman, J., Stanley, K. O., and Clune, J. (2019). Go-explore: a new approach for hard-exploration problems. *arXiv preprint arXiv:1901.10995*.

Gu, S., Lillicrap, T., Sutskever, I., and Levine, S. (2016). Continuous deep q-learning with model-based acceleration. In *International conference on machine learning*, pages 2829–2838. PMLR.

Janz, D., Hron, J., Mazur, P., Hofmann, K., Hernández-Lobato, J. M., and Tschiatschek, S. (2019). Successor uncertainties: exploration and uncertainty in temporal difference learning. *Advances in Neural Information Processing Systems*, 32.

Kononenko, I. (1989). Bayesian neural networks. *Biological Cybernetics*, 61(5):361–370.

Liu, Y., Chen, J., and Chen, H. (2018). Less is more: Culling the training set to improve robustness of deep neural networks. In *International Conference on Decision and Game Theory for Security*, pages 102–114. Springer.

Liu, Y., Ding, J., and Liu, X. (2020a). A constrained reinforcement learning based approach for network slicing. In *2020 IEEE 28th International Conference on Network Protocols (ICNP)*, pages 1–6. IEEE.

Liu, Y., Ding, J., and Liu, X. (2020b). Ipo: Interior-point policy optimization under constraints. In *Proceedings of the AAAI Conference on Artificial Intelligence*, volume 34, pages 4940–4947.

Liu, Y., Ding, J., and Liu, X. (2021a). Resource allocation method for network slicing using constrained reinforcement learning. In *2021 IFIP Networking Conference (IFIP Networking)*, pages 1–3. IEEE.

Liu, Y., Ding, J., Zhang, Z.-L., and Liu, X. (2021b). Clara: A constrained reinforcement learning based resource allocation framework for network slicing. In *2021 IEEE International Conference on Big Data (Big Data)*, pages 1427–1437. IEEE.

Liu, Y., Halev, A., and Liu, X. (2021c). Policy learning with constraints in model-free reinforcement learning: A survey. In *The 30th International Joint Conference on Artificial Intelligence (IJCAI)*.

Liu, Y. and Liu, X. (2021). Cts2: Time series smoothing with constrained reinforcement learning. In *Asian Conference on Machine Learning*, pages 363–378. PMLR.

Liu, Y. and Liu, X. (2023a). Adventurer: Exploration with bigan for deep reinforcement learning. *Applied Intelligence*.

Liu, Y. and Liu, X. (2023b). Constrained reinforcement learning for autonomous farming: Challenges and opportunities. In *AI for Agriculture and Food Systems*.

Lu, L., Liu, L., Hussain, M. J., and Liu, Y. (2017). I sense you by breath: Speaker recognition via breath biometrics. *IEEE Transactions on Dependable and Secure Computing*, 17(2):306–319.

Lu, L. and Liu, Y. (2015). Safeguard: User reauthentication on smartphones via behavioral biometrics. *IEEE Transactions on Computational Social Systems*, 2(3):53–64.

Metelli, A. M., Likmeta, A., and Restelli, M. (2019). Propagating uncertainty in reinforcement learning via wasserstein barycenters. *Advances in Neural Information Processing Systems*, 32.

Mnih, V., Badia, A. P., Mirza, M., Graves, A., Lillicrap, T., Harley, T., Silver, D., and Kavukcuoglu, K. (2016). Asynchronous methods for deep reinforcement learning. In *International conference on machine learning*, pages 1928–1937. PMLR.

Mnih, V., Kavukcuoglu, K., Silver, D., Rusu, A. A., Veness, J., Bellemare, M. G., Graves, A., Riedmiller, M., Fidjeland, A. K., Ostrovski, G., et al. (2015). Human-

level control through deep reinforcement learning. *Nature*, 518(7540):529.

Osband, I., Van Roy, B., and Wen, Z. (2016). Generalization and exploration via randomized value functions. In *International Conference on Machine Learning*, pages 2377–2386. PMLR.

O'Donoghue, B., Osband, I., Munos, R., and Mnih, V. (2018). The uncertainty bellman equation and exploration. In *International Conference on Machine Learning*, pages 3836–3845.

Qu, H., Xie, X., Liu, Y., Zhang, M., and Lu, L. (2015). Improved perception-based spiking neuron learning rule for real-time user authentication. *Neurocomputing*, 151:310–318.

Rasmussen, C. E. (2003). Gaussian processes in machine learning. In *Summer school on machine learning*, pages 63–71. Springer.

Tesauro, G. et al. (1995). Temporal difference learning and td-gammon. *Communications of the ACM*, 38(3):58–68.

Van Hasselt, H., Guez, A., and Silver, D. (2016). Deep reinforcement learning with double q-learning. In *Proceedings of the AAAI conference on artificial intelligence*, volume 30.

Yang, E. and Gu, D. (2004). Multiagent reinforcement learning for multi-robot systems: A survey. Technical report, tech. rep.

Yang, T., Tang, H., Bai, C., Liu, J., Hao, J., Meng, Z., and Liu, P. (2021). Exploration in deep reinforcement learning: a comprehensive survey. *arXiv preprint arXiv:2109.06668*.

Zhu, Z., Bıyık, E., and Sadigh, D. (2020). Multi-agent safe planning with gaussian processes. In *2020 IEEE/RSJ International Conference on Intelligent Robots and Systems (IROS)*, pages 6260–6267. IEEE.

APPENDIX

EMPIRICAL RESULTS

As stated in the paper, Farsighter can work on a wide range of RL tasks with high/low-dimensional states, discrete/continuous actions, and sparse/dense rewards. We show the performance for sparse reward tasks in the main paper. In Table 2 and 3, we show the performance for all the atari games and dense reward continue task(Walker2D), where Farsighter outperforms the SOTA.

PSEUDOCODE FOR CONTINUOUS TASKS

The pseudocode for continuous one-step uncertainty driven Q-Learning is shown in Alg. 3. To extend

---

Algorithm 3: Continuous one-step uncertainty driven Q-Learning with NAF.

Given NAF, we have
$Q(s,a|\theta^Q) = A(s,a|\theta^A) + V(s|\theta^V);$
$A(s,a|\theta^A) = -\frac{1}{2}(a - \mu(s|\theta^a))^T P(s|\theta^P)(a - \mu(s|\theta^a))$
and BNN $\mu(s|\theta^{va})$
Randomly initialize normalized Q network and BNN
Initialize target network Q' with weight $\theta^{Q'} \leftarrow \theta^Q$
Initialize replay buffer R

1: **for** episode=1, M **do**
2:     Receive initial observation state s_1
3:     **for** t = 1,T **do**
4:         Select a variance ε from BNN layer $\mu(s|\theta^{va})$ and action $a_t = \mu(s|\theta^a) + \varepsilon$
5:         Execute a_t and observe r_t and s_{t+1}
6:         Store transition (s_t, a_t, r_t, s_{t+1}) into R
7:         **for** iteration=1,I **do**
8:             Sample a random minibatch of m transitions from R
9:             Update $\theta^a, \theta^V, \theta^P$ as normal NAF with fixing θ^{va}.
10:           Every M steps: Update the BNN layer $\mu(\phi(s)|\theta^{va})$
11:           Every N steps: Update the target network: $\theta^{Q'} \leftarrow \tau\theta^Q + (1-\tau)\theta^{Q'}$
12:     **end for**
13:     **end for**
14: **end for**

---

the process to multi-step, we can recursively deploy Thompson sampling on the BNN layer of $\mu(\phi(s)|\theta^{va})$ to get multi-step samples, which is similar with Alg. 2 in the main paper.

EXPERIMENT DETAILS

Network Architecture

Discrete Action Tasks

For discrete action tasks, the input observations are raw images (e.g., Atari games). The input to the network is $4 \times 84 \times 84$ tensor with a re-scaled and averaged over channels of the last four observations. The first convolution layer has 32 filters of size 8 with a stride of 4. The second convolution layer has 64 filters of size 4 with stride 2. The last convolution layer has 64 filters of size 3 followed by a fully connected layer of size 512.

Table 1: Hyperparameters.

Hyperparameter	Value
Number of Seeds	10
Optimizer	RMSProp
Learning rate	0.0025
Momentum	0.95
Discount factor	0.99
Representation network update frequency	4 steps
Representation network update mini-batch	32 tuples
Target network update frequency (N)	10k steps(Atari Games); 1k (Robotic controls)
Posterior update frequency (M)	10*N;
Posterior update mini-batch	100k tuples(Atari Games); 1k tuples(Robotic controls)
BLR noise variance σ_ε	1
BLR prior variance σ	0.1
Replay buffer size	1M tuples

Continuous Action Tasks

For continuous action tasks, the input observations are low dimensional sensor data (e.g., robotic control). The inputs are different from domain to domain. We use two fully connected layers with hidden size 64 and 32 for the representation layer, which works in general for different continuous domains.

Hyper-Parameters

In table 1, we show the hyper-parameters for the algorithms to run. We randomly initialize the parameters of the networks. Since our methods are based on DDQN (NAF), most hyper-parameters are equivalent to ones in DDQN(NAF) setting. To optimize for this set of hyper-parameters we set up a simple, fast, and cheap hyper-parameter tuning procedure. For example, for Atari Games, we used a pre-trained DDQN model for the game of Montezuma's Revenge, and removed the last fully connected layer in order to have access to its already trained state representation. Then we tried combination of $M = \{N, 10*N\}, \sigma = \{1, 0.1, 0.001\}$, and $\sigma_\varepsilon = \{1, 10\}$ and test for 10000 episodes of the game. The procedure is cheap and fast since it requires only a few times of posterior update. We set these parameters to their best $M = 10*N, \sigma = 0.1, \sigma_\varepsilon = 1$.

COMPLEXITY ANALYSES

Farsighter vs BDQN (One-step Bayesian NAF): As mentioned Sec. 4.4, we did not change the update rule for multi-step updates. We only change the data samples used to do the optimization. So Farsighter would not change the computation cost compared to BDQN

(One-step Bayesian NAF). Moreover, multi-step updates store the sum of discounted rewards and final states after k steps to the replay buffer. The transmission tuples are in the same format with one-step updates, thus Farsighter would not increase the memory complexity either.

BDQN vs DDQN: For a given period of game time, the number of the backward pass in both BDQN and DQN are the same whereas for BDQN it is cheaper since there is no backward pass for the final layer. BDQN has more forward passes compared with DDQN. To update the posterior distribution, BDQN draws samples from the replay buffer and needs to compute their feature vectors, as it is mentioned in Sec. 4.2,The increased number is based on the update frequency and posterior update batch size. One can easily relax it by parallelizing this step along the main body of BDQN or deploying online posterior update methods.

One-step Bayesian NAF vs NAF: The update of the BNN layer $\mu(\phi(s)|\theta^{va})$ is complex then a liner layer. While for continuous action tasks the dimension of BNN layer is low thus it is easy to train. As mentioned in the Sec. 6, the input dimension for the BNN layer is 32. Empirically, we run experiences on Fetch Pick And Place task. The running time is similar for both cases, which is around six hours.

In summary, we would not increase the computational and memory cost. Farsighter can work appropriately in complex real-world domains.

Table 2: Raw scores for Atari games. The performance of OB2I is from (Bai et al., 2021).

	Farsighter	DDQN	BDQN	OB2I(20M)
Alien	3762.50	1620.00	3167.20	916.90
Amidar	1934.20	978.00	1815.30	94.00
Assault	7439.30	4280.40	5439.40	2996.20
Asterix	39556.40	4359.00	44438.30	2719.00
Asteroids	2603.70	1364.50	2363.20	959.90
Atlantis	3959257.80	279987.00	2823842.40	3146300.00
Bank Heist	983.70	455.00	834.50	378.60
Battle Zone	47936.70	29900.00	45348.40	13454.50
Beam Rider	19504.80	8627.50	9456.30	3736.70
Bowling	54.62	50.40	38.40	30.00
Boxing	91.77	88.00	79.30	75.10
Breakout	597.20	385.50	392.60	423.10
Centipede	5936.10	4657.70	7134.70	2661.80
Chopper Command	13940.60	6126.00	17363.60	1100.30
Crazy Climber	149507.70	110763.00	137693.80	53346.70
Demon Attack	32233.61	12149.40	23595.40	6794.60
Double Dunk	3.50	-6.60	-1.30	-18.20
Enduro	1604.70	729.00	1496.50	719.00
Fishing Derby	3.80	-4.90	27.30	-60.10
Freeway	48.02	30.80	30.10	32.10
Frostbite	1795.30	797.40	1643.60	1277.30
Gopher	19418.90	8777.40	13742.80	6359.50
Gravitar	1175.81	473.00	589.30	393.60
H.E.R.O.	22010.70	20437.80	21532.70	3302.50
Ice Hockey	-0.70	-1.90	-2.70	-4.20
James Bond	1707.25	768.50	1593.70	434.30
Kangaroo	14651.80	7259.00	13596.30	2387.00
Krull	13263.91	8422.30	9643.60	45388.80
Kung-Fu Master	38734.99	26059.00	40563.70	16272.20
Montezumas Revenge	413.60	0.00	0.00	0.00
Ms. Pac-Man	3796.19	3085.60	3295.50	1794.90
Name This Game	12312.80	8207.80	10536.70	8576.80
Pong	20.25	19.50	19.80	18.70
Private Eye	494.50	146.70	149.70	1174.10
Q*Bert	20788.47	13117.30	19530.60	4275.00
River Raid	12597.50	7377.60	15830.10	2926.50
Road Runner	55823.20	39544.00	51062.70	21831.40
Robotank	66.61	63.90	60.70	13.50
Seaquest	6880.48	5860.60	7934.70	332.10
Space Invaders	5684.02	1692.30	7830.80	904.90
Star Gunner	96013.91	54282.00	79403.70	1290.20
Tennis	19.10	12.20	-1.00	-1.00
Time Pilot	6402.11	4870.00	7932.70	3404.50
Tutankham	201.70	68.10	230.60	297.00
Up and Down	17328.92	9989.90	23056.90	5100.80
Venture	951.36	163.00	693.80	16.10
Video Pinball	529524.60	196760.40	47246.80	80607.00
Wizard Of Wor	7429.40	2704.00	9450.80	480.70
Zaxxon	8934.95	5363.00	8394.70	2842.00

Table 3: The score for dense reward continue tasks (30k steps).

	NAF	Multi-step NAF	Bayesian NAF	Farsighter
Walker2D	-75.8 ± 631.0	-68.2 ± 649.0	160.1 ± 493.0	230.2 ± 566.8